An Interactive Algorithm for Image Denoising and Segmentation

MARCOS C. DE ANDRADE [1] BABA C. VEMURI [2]

[1] Centro de Desenvolvimento da Tecnologia Nuclear - CDTN, P.O. BOX 941, Belo Horizonte, MG, Brazil
mca@cdtn.br
[2] Computer and Information Sciences and Engineering – CISE – University of Florida, Gainesville, FL, USA
vemuri@cise.ufl.edu

Abstract. This paper presents an interactive algorithm for image denoising and segmentation. A global competition criterion is used to impose an order of processing on all image pixels. The smoothing step employs an evolution equation controlled by the local curvature to denoise the image while preserving the features. The interactive segmentation step requires the user to select one definitive seed per region. Region growing is initiated around provisory seeds, which are automatically detected, labeled and eventually merged by the algorithm. A simple merging mechanism is used to handle the topological transformations required to remove the image over-segmentation. It is shown that accurate and fast segmentation results can be achieved for gray and color images using this simple method. Extension to 3D images is straightforward and easily handled.

Keywords: Image segmentation, PDE, watershed, image denoising, deformable models, snakes, region growing.

1. Introduction

Image denoising and segmentation play an important role in image analysis and computer vision. Image denoising reduces the noise introduced by the image acquisition process while image segmentation recovers the regions associated to the objects they represent in a given image. These treatments typically rely on semantically poor information, directly obtained from the image around a spatially restrained neighborhood and, for this reason, are broadly classified as *low-level* treatments [8].

Image segmentation often requires pre- and post-processing, where the user judgment is fundamental and helps to feed information of high semantic content back into the process. The pre-processing is an essential step in which specialized filters smooth the image simplifying it for the subsequent segmentation step. Interactive segmentation allows the user to intervene directly in the segmentation contributing to its success. Post-processing may be required to complete the task if the segmentation itself fails to produce the desired results.

Image segmentation is an application-oriented problem. There is no general-purpose segmentation method. The choice of a particular technique depends on the nature of the image (non-homogeneous illumination, presence of noise or texture, ill-defined contours, occlusions), post-segmentation operations (shape recognition, interpretation, quality control, localization, measurements), primitives to be extracted (contours, straight segments, regions, shapes, textures) and on physical limitations (algorithmic complexity, real-time execution, available memory) [8]. It is not possible to define, a priori, how good a segmentation method is. The quality of a segmentation method can be evaluated by the results obtained from the treatments using the extracted primitives.

Other important issues concerning fundamental aspects of image segmentation methods are initialization, convergence, ability to handle necessary topological changes, stopping criteria and over-segmentation.

Segmentation by *deformable models* (DM) describes contours, which evolve under a suitable energy functional. In the pioneer work of Kass et. al., the *snakes* method [20], image forces and external constraints guide the evolution of the DMs by minimizing the energy of spline curves and surfaces. Former versions of the *snakes* method required the initialization to be done close to the boundaries of the objects to guarantee proper convergence and to avoid being trapped by local minima. Recent versions of the *snakes* method [29] solved this problem. The *balloon* method [14] adds an inflation force to the snakes to move the initialized model into the neighborhood of the edges avoiding the local minima. However, the inflation force often pushes the contour over weak edges.

Modeling the contours in the level set framework [9,10] easily solves the topological problem, i.e., merge the non-significant curves. The *active contours* method [5] presented by Caselles et. al. and the *front propagation*

method [23,24] introduced by Malladi et. al. greatly simplify the topological problem but do not address the initialization and convergence issues. Initialization is usually difficult and time-consuming requiring the manual introduction of polygons around the features of interest. Convergence is also difficult since some models are still evolving while others have finished the evolution or, worse, have leaked through weak boundaries. The geometrical version of the *active contours* method is stable and retrieve simultaneously several contours but do not retrieve angles [5].

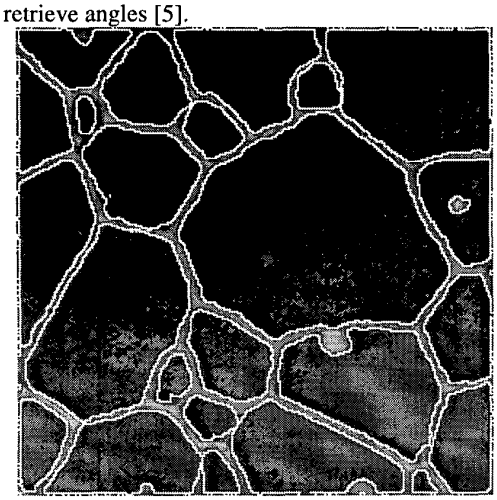

Figure 1. Convergence is difficult to achieve using the bubbles method [7] implemented in the PDE based level set framework.

The *bubbles* method [7] simplifies the initialization issue allowing, for instance, the contours to be initialized at the image minima or at predefined grid cells having homogeneous statistical properties. However, the *bubbles* method depends on fine tuning parameters in order to achieve simultaneous convergence of bubbles and is slow compared to the *watershed* based methods. Figure 1 illustrates the convergence problem using the *bubbles* method on a ceramic micrographs containing grains separated by thin gaps. In this example the bubbles were initialized at the image minima. Notice that some bubbles have converged while others are still evolving and some are being merged.

Conventional region growing and merging methods work well in noisy images but are sensitive to seed initialization and produce jagged boundaries. The *Seeded region growing* method (SRG) [1, 22] introduces a competition between by ordering all pixels according to some suitable criteria, a property inherited from the *non-hierarchical watershed* method [15,16]. This global competition ensures that the growth of regions near the weak or diffused edges is delayed until other regions have had a chance to reach these areas. SRG does not incorporate any geometric information and hence can leak through narrow gaps or weak edges, as illustrates Figure2.

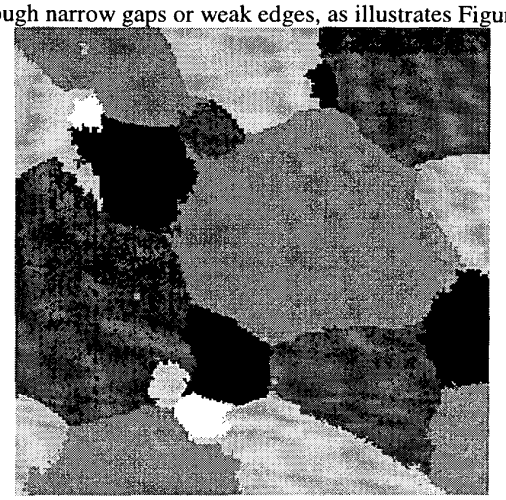

Figure 2. Seeded Region Growing – SRG can leak through weak or diffused edges

The region competition method – (RC) [27] combines the geometrical features of the DM and the statistical nature of SRG. It introduces a local competition between regions by trading pixels that result in a decrease in energy, thus allowing recovery from errors. However, RC produce jagged boundaries and depends on seed initialization which eventually leads to leakage through weak boundaries if the seeds are asymmetrically initialized [28].

The *non-hierarchical watershed* method – (NHW) treats the image as a surface, starts the region growing from the surface minima and expands them following *geodesic paths*, thus minimizing the potential energy. The region growing process continues until neighbor regions touch each other. This provides a powerful stopping criterion difficult to achieve in the PDE based level set framework. However, NHW leads to a strong over-segmentation if proper image smoothing is not provided. Alternative solutions to the NHW over-segmentation exist [17, 18, 19], however, they require the fine-tuning of parameters related to geometric features of the regions.

The hierarchical watershed method - (HW) starts the region growing process from markers. Usually, highly specialized filters are required to select the markers. HW is optimal from the point of view of the execution time. Finally, the *skeletally coupled deformable models* method (SCDM) [28] combines features of curve evolution deformable models as *bubbles* and *region-competition* and introduces an inter-seed skeleton to mediate the segmentation. Nonetheless, it requires an elaborated sub-pixel implementation using ENO schemes [13, 28].

This paper introduces an interactive algorithm for image denoising and segmentation – (IIDSA) which retains some of the most attractive features of the methods described above and overcomes some of their limitations.

It combines a noise removal step and an interactive image segmentation step in one algorithm, resulting in a robust and easy-to-use tool where higher level knowledge of the image can readily be incorporated in the segmentation process. IIDSA provides solutions to automatic initialization and stopping criterion, convergence and over-segmentation. However, it does not handle region shrinking or splitting.

2. The interactive image denoising and segmentation algorithm

The interactive image denoising and segmentation algorithm – (IIDSA) treats the image as 3D surfaces in evolution. This construction serves a dual purpose: first, a denoising filter, which efficiently preserves edges, is implemented in the PDE based level set framework [9, 10] constraining the surface to evolve according to its vertically projected mean curvature [2, 12], see section 3.1. Secondly, an efficient segmentation algorithm, avoiding the costly PDE, is implemented in the Mathematical Morphology framework [3, 4, 15, 16, 17, 18, 19, 25, 26]. In this context, the segmentation is an ordered region-growing and merging process initiated at the minima of the surface whose evolution is constrained by geodesic paths imposed by the surface itself, see section 3.2.

The IIDSA segments the image into as many regions as the number of seeds interactively selected by the user, here called definitive seeds to distinguish them from the provisory seeds automatically detected by the algorithm. Initiating the region growing around the image minima (white dots shown in Figure 3a), makes the algorithm less sensitive to seed (black spots) positioning or seed size.

The topological transformations required to reduce the over-segmentation are easily handled through a simple merging mechanism. However, the IIDSA has no provision for region splitting and thus no region shrinking.

Figure 3a shows a micrograph of ceramic sample containing gains (dark gray) separated by thin edges (light gray), *definitive seeds* selected by the user (black spots) and *provisory seeds* automatically detected by the algorithm (white dots). Figure 3b shows the regions of influence associated to each minima of the original image. Figure 3c shows the IIDSA segmentation result after merging the non-significant regions.

The IIDSA is an interactive algorithm, and so requires the user to add and subtract seeds and to repeat the process until the desired results can be achieved. Making the segmentation interactive allows some high level knowledge of the image to be feedback into the process, thus improving the segmentation results.

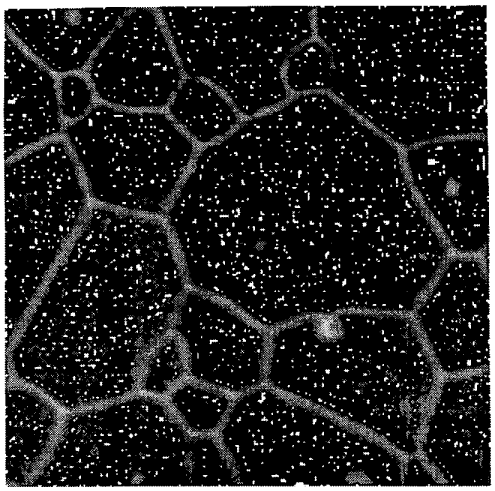

Figure 3a. Seeds superimposed on the original image

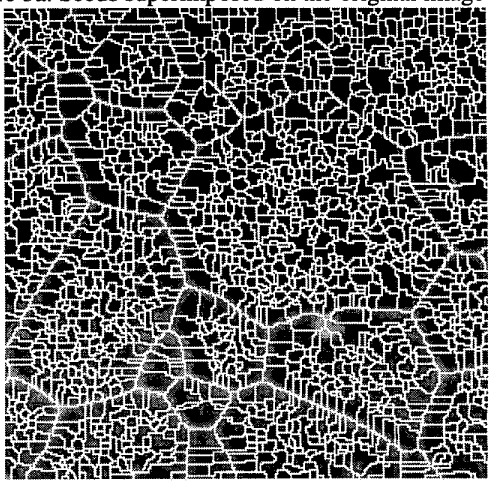

Figure 3b. Zones of influence of each minimum

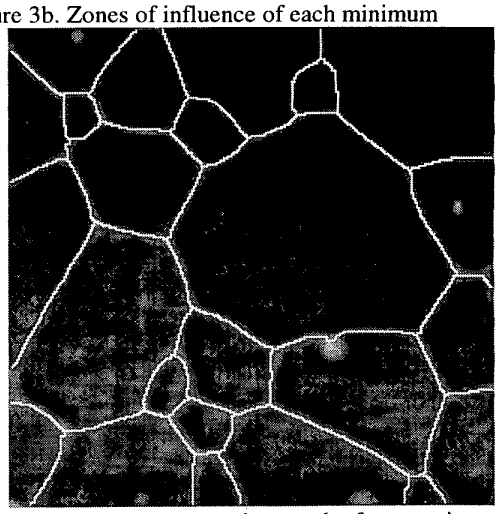

Figure 3c. IIDSA segmentation result after merging.

2.1 Edge preserving smoothing under controlled curvature motion

Surface evolution under the PDE based level set framework [9, 10] has been successfully used to perform both image denoising and image segmentation. For image denoising purposes, partial differential equations (PDEs) can be employed to modify the image topology and implement an edge preserving smoothing under controlled curvature motion [2, 12].

By treating the image *I(x,y,z(t))* as a time-dependent surface in R and selectively deforming the surface based on the vertical projection of its mean curvature, effectively removes most of the non-significant image's extrema. For smoothing purposes the surface height z at the point *p(x,y)* is initialized as value of the local gray-level. The local surface deformation is computed from the local mean curvature κ expressed by the following relation between the second derivatives of *I*:

$$\kappa = \frac{I_{xx}(1+I_y^2) - 2I_x I_y I_{xy} + I_{yy}(1+I_x^2)}{2(1+I_x^2+I_y^2)^{3/2}} \qquad (1)$$

Evolving the image I, as a surface, under this modified level set curvature motion is equivalent to repeatedly iterating the following edge-preserving anisotropic filter:

$$I_{t+1} = I_t + \kappa \qquad (2)$$

Figure 4 illustrates the results of applying the anisotropic filter to a corneal endothelial cell for 20, 40 and 60 iterations respectively. After 60 iterations most of the noise has been attenuated.

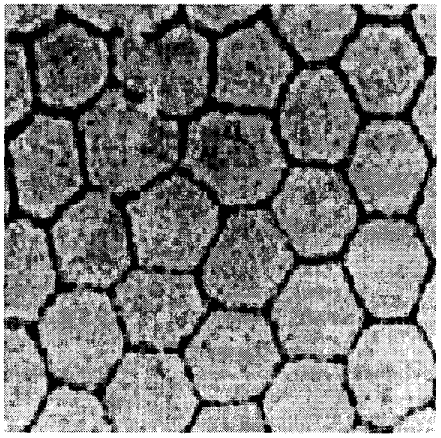

Figure 4a. Original endothelial cells

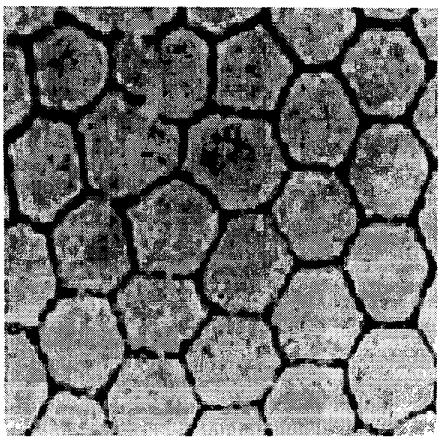

Figure 4b. Smoothing after 20 iterations

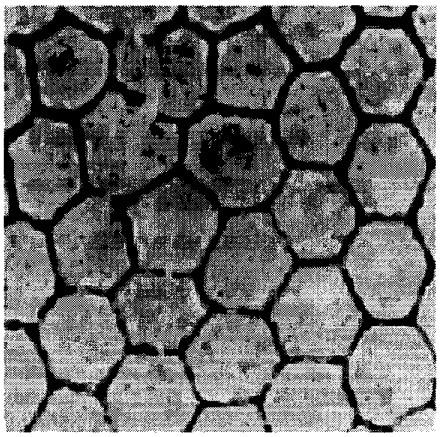

Figure 4c. Smoothing after 40 iterations

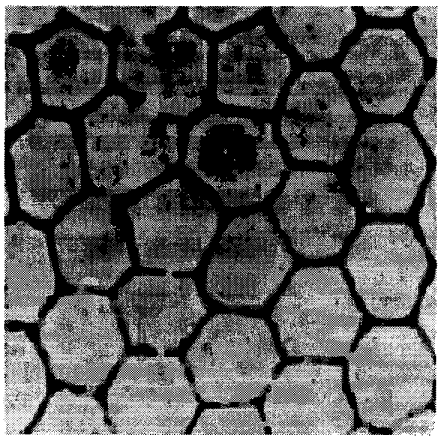

Figure 4d. Smoothing after 60 iterations

2.2 The interactive region growing and merging step

In region-growing methods the growing process is initiated around seeds located in the inner parts of the regions and follows a given "order of processing".

Usually, the regions grow in successive layers until the growing process finally stops thus defining the definitive location of the edges. From this perspective, the most important pixels are precisely those located in a narrow-band around the definitive location of the edges. Sorting all image pixels according to a convenient relation between each pixel *p(x,y)* and its neighborhood NP, is sufficient to impose an "order of processing", deferring the processing of pixels on the edges. This ordering can be established, for instance, defining a 3D surface whose height z, at each point *p(x,y)*, is computed from this relation. Sorting the z's in ascending order allows the region-growing process to automatically start from the minima of this surface. The following relations, for instance, were implemented in the IIDSA:

- In its simplest form, z is assigned to the value of the image's gray-levels themselves;
- z can be the difference between a pixel and mean value in N(p) as in the SRG method;
- the difference between the maximum and the minimum values in N(p);
- the mean curvature at p(x,y) as expressed by equation 2.

The first relation is useful when the image characteristics are such that the gray-levels themselves already dictate a natural order of processing. An example is shown in Figure 3b, which already have edges at *higher* elevation than the inner parts. The second is useful for images having homogeneous textures. The third criterion is useful, for instance, in images having a stepwise transition between the regions as shown in Figure 7. In this case, taking the difference between the maximum and the minimum in N(x), forces higher values at the edges and have the additional benefit of closing small gaps in the borders.

Finally, adding a merging mechanism, controlled by user-selected seeds, the region growing and merging is complete. A simple table, as shown in Table 1, can be used to merge the regions. This table is initialized as a sequence of integer numbers from I to N, where N is at least equal to the number of minima present in the image. This table is updated according to the sequence of absorptions. If, for instance, the region having label = 1 absorbs the region having label = 3, the merging table is updated as shown below:

before	1	2	3	4	5	...	i	...	N
after	1	2	1	4	5	...	i	...	N

2.3 The IIDSA algorithm

The IIDSA algorithm is outlined below.

1. Apply the edge preserving anisotropic filter (eq. 2), to the image.

2. Using a mouse, place one seed per region, labeling them from 1 to N. The user-selected seeds are here referred to as *definitive seeds* to distinguish them from the *provisory seeds* detected by the algorithm. They may be a single point or sets of points inside a user-selected polygon.

3. Sort all image pixels, in ascending order, by the address calculation technique described in [11] according to one of the criteria listed below:

- gray-level value of the current pixel;
- difference between the maximum and minimum values in a neighborhood N(p) of the current pixel;
- difference between a pixel and the mean of it's neighbors;
- mean curvature at the current pixel;
- any other criteria which can be used to defer the processing of the edges.

4. For each sorted pixel *p*, extracted from the sorted list, find how many labeled pixels exist in its neighborhood N(p). The three possible outcomes are: There is no labeled pixel in N(p). The current pixel receives a new label and starts a new provisory region. New regions receive labels starting from N+1. These labels are here referred to as provisory labels and are assigned to *provisory seeds.* There is only one labeled pixel in N(p). The current pixel receives this label and is integrated into the neighbor region. There are more than one labeled pixels in N(p). If two or more neighbors have definitive seeds (label <= N) a real border has been found, mark the current pixel as a "border", say a -1 label, else merge all neighbors into one region (the one having the smaller label; the first labeled in N(p)) and add the current pixel to it.

5. Re-label all pixels to reflect the absorption they have undergone using a merging table.

6. Draw the segmented image according to the newly assigned labels.

Figure 5, illustrates the IIDSA merging process for an x-ray image. Since this image contains regions whose transitions are stepwise, the gray levels cannot be directly used to impose an order of processing to the pixels. The difference between the maximum and minimum values in N(p) was used, instead.

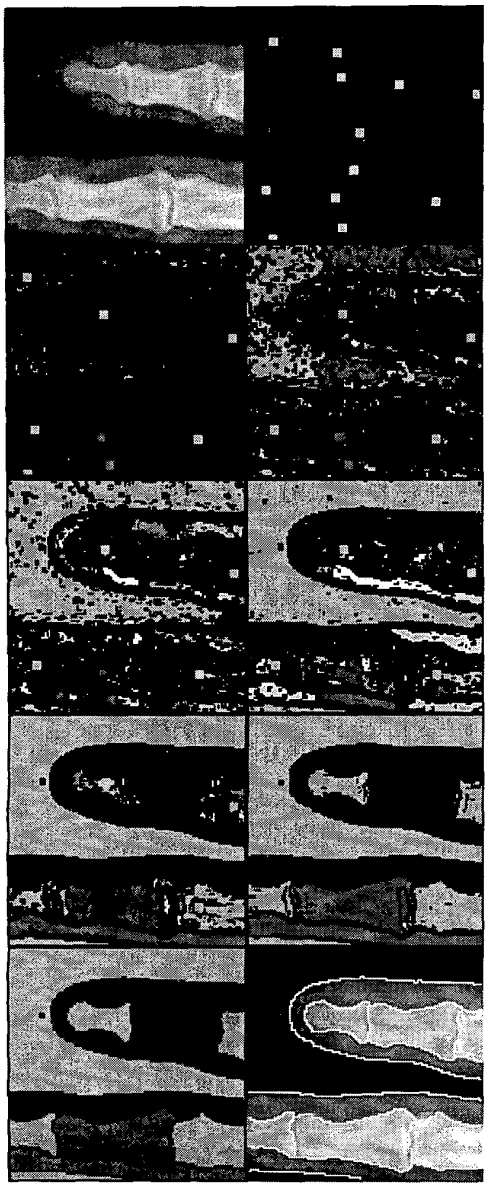

Figure 5. Snapshots for increasing time-steps.

3. Application to micrographs

This section illustrates some practical results produced by the IIDSA algorithm. Figure 6a shows a ceramic micrograph containing grains (darker regions) separated by thin gaps (lighter regions). The highlighted areas in Figure 6a indicate weak/diffused boundaries. One 3x3 seed per region was marked inside each region. Since the borders already have gray-levels higher than the grains, *all* pixels were sorted according to the gray level criterion. In this case, a complete tessellation of the space is required to segment the image. Figure 6b shows the IIDSA segmentation result. Notice that even the barely perceptible edges have been correctly detected. Figure 7a shows a micrograph of albitite, a geological material, containing grains. In this image, the difference between maximum and minimum values in N(p) was used to sort the image pixels, forcing higher values at the edges. Figure 7b shows the IIDSA segmentation result. Observe that some "leaking" occurred parallel to the edges in homogeneous flat zones. Figure 8 shows the *definitive seeds* (black spots) and the IIDSA segmentation result (white lines) superimposed on the original cross-section of a human renal glomerulus. The sorting criterion was based on the maximum-minimum difference in N(p) forcing higher values at the edges. Only a few seeds (one per region) were needed to extract the edges of the main structures.

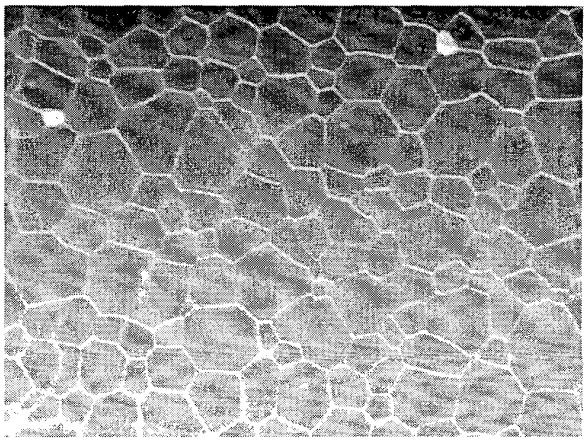

Figure 6a. Original micrograph of ceramic material

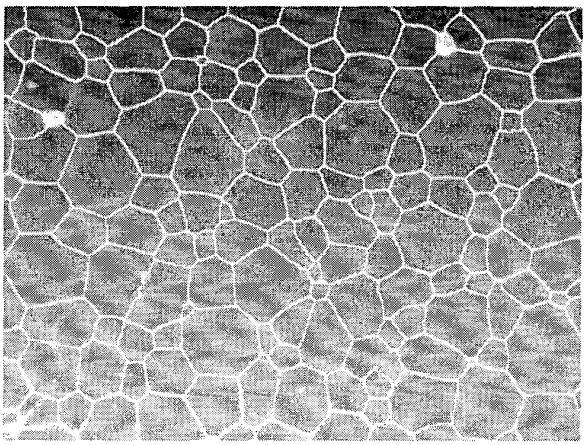

Figure 6b. IIDSA segmentation result.

4. Concluding remarks

The IIDSA combines some valuable features of known image smoothing and segmentation methods developed in the Mathematical Morphology and in the PDE based Level Set frameworks.

Figure 7a. Original micrograph of albitite

Figure 7b. Seeds and the IIDSA segmentation result

For instance, efficient edge preserving smoothing guided by PDEs, typical of surface evolution methods; ability to automatically detected all image minima and to make the regions grow inside geodesic domains, a property inherited from the *watershed* transformation; ability to automatically stop the growing process whenever two user selected regions touch each other, a characteristic difficult to implement in the PDE based level set framework; global competition between all image pixels according to a user selected criteria; ability to change the image topology using a simple merging mechanism, thus dramatically reducing the over-segmentation; recovery from errors mediated by a user guided segmentation; low sensitivity to seed positioning and execution time directly proportional to image size. However, the IIDSA does not provide region splitting and shrinking. At the expense of more user interaction, the IIDSA allows the recovery of complex shapes from images in 2D or 3D in gray-scale or color images. The algorithm can be easily extended to n-dimensional images. For the future efforts will be directed to improve the merging algorithm. An attribute based splitting mechanism is also being considered.

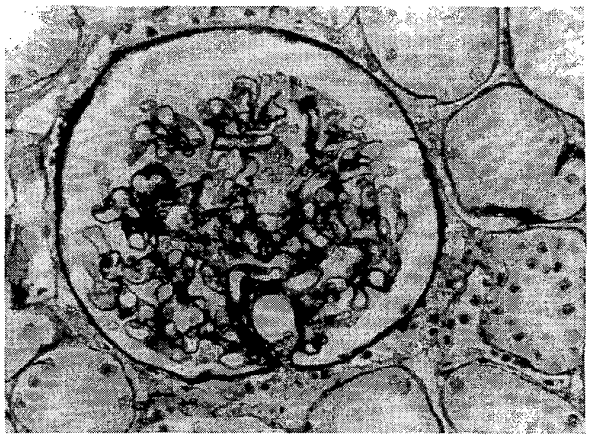

Figure 8a. Original micrograph of a renal glomerulus

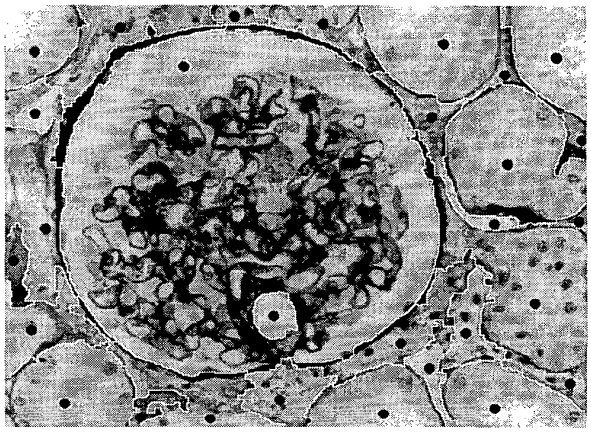

Figure 8b. Seeds and IIDSA segmentation result

5. Acknowledgments

The first author would like to acknowledge the CNPq - Conselho Nacional de Desenvolvimento Científico e Tecnológico, and the CISE - Computer and Information Sciences and Engineering of the University of Florida, for the financial and technical support

6. References

[1] A. Mehnert et. al., An improved seeded region growing algorithm. *Pattern Recognition Letters, 18,* (1997), 106-1071.

[2] A. Yezzi, Modified curvature motion for image smoothing and enhancement. *IEEE Trans. on Image Processing,* 7, 3, (1998), 345-352.

[3] F. Meyer and S. Beucher, Morphological segmentation. *Journal of Visual Communication and Image Representation, 1, 1, (1990), 21-46.*

[4] F. Meyer. Un algorithme optimal de ligne de partage des eaux. VIII Congrès de *Reconaissance de Forme et d'Intelligence Artificielle.* Lyon, France, (1991), 847-857.

[5] F. Caselles et al. Image selective smoothing and edge detection by nonlinear diffusion. *SIAM Journal on Numerical Analysis,* 29, 1, (1992), 183--193.

[6] G. Guo et. al. Bayesian learning, global competition and unsupervised image segmentation. *Pattern Recognition Letters,* 21, (2000), 107-416.

[7] H. Tek et. al. Volumetric segmentation of medical images by three-dimensional bubbles. *Computer Vision and Machine Understanding,* 65, 2, (1997), 246--258.

[8] J. P. Cocquerez and S. Philipp, *Analyse d' images: filtrage et segmentation.* Masson, Paris, (1995).

[9] J. A. Sethian Level Set Methods and Fast Marching Methods. Cambridge Press, 2nd ed., (1999).

[10] J. A. Sethian Tracking Interfaces with Level Sets. *American Scientist,* may-jun (1997).

[11] J. Isaac et al. Sorting by Address Calculation. *Journal of the ACM,* (1954), 169--174

[12] J. Weickert. *Anisotropic diffusion in image processing. B.G.* Teubner Sttutgart, Deutschland, (1998).

[13] K. Siddiqi et. al. Geometric shock-capturing ENO schemes for sub-pixel interpolation, computation and curve evolution. *Graphical Models and Image Processing,* 59, 5, (1997), 278--301.

[14] L. D. Cohen at. al. Finite element methods for active contours models and balloons for 2D and 3D images. *IEEE Trans. Pattern Analysis and Machine Intelligence,* 15, (1993), 1131--1147.

[15] L. Vincent and P. Soille, Watersheds in digital spaces: An efficient algorithm based on immersion simulations. *IEEE Trans. Pattern Analysis and Machine Intelligence,* 13, 6, (1991), 583--598.

[16] L. Vincent, *Algorithmes morphologiques a base de files d'attente et de lacets Extension aux graphes.* École Nationale Supérieure de Mines de Paris, PhD thesis, (1990).

[17] M. C. Andrade et. al. Segmentation of microscopic images by flooding simulation: a catchment basins merging algorithm. *Proceedings of SPIE Nonlinear Image Processing VIII,* San Jose, USA, 3026, (1997), 164--175.

[18] M. Grimaud, A new measure of contrast: the dynamics. *Proceedings of SPIE. Image Algebra and Morphological Image Processing,* 1769, (1992).

[19] M. Grimaud, *La geodesie numerique en morphologie mathematique. Application a la detection automatique de microcalcifications en mammographie numerique,* École Nationale Supérieure de Mines de Paris, PhD thesis, (1991).

[20] M. Kass et. al. Snakes Active Contour models. *International Journal of Computer Vision, 1,* (1988), 321-331.

[21] P. Perona et. al. Scale-space and edge detection using anisotropic diffusion. *IEEE Trans. Pattern Analysis and Machine Intelligence. 12,* 7, (1990), 629--639.

[22] R. Adams et. al. Seeded region growing. *IEEE Trans. Pattern Analysis and Machine Intelligence,* 16, 6, 641-647, (1994).

[23] R. Malladi et al. A fast level set based algorithm for topology-independent shape modeling. *Journal of Mathematical Vision,* 6, (1996), 269-289.

[24] R. Malladi et al. Shape modeling with front propagating: a level set approach. *IEEE Trans. Pattern Analysis and Machine Intelligence,* 17, 2, (1995), 158--175.

[25] S. Beucher. *Segmentation d'image et morphologie mathematique.* École Nationale Supérieure de Mines de Paris, PhD thesis, (1990).

[26] S. Beucher. Watershed, hierarchical segmentation and waterfall algorithm. *Mathematical Morphology and its Applications to Image Processing,* 69--76, Kluwer Academic Publishers, (1994).

[27] S. C. Zhu et al. Region competition: unifying snakes, region growing, and bayes/MDL for multiband image segmentation, *IEEE Trans. Pattern Analysis and Machine Intelligence,* 18, 9, (1996), 880--900.

[28] T. Sebastian et. al. Segmentation of carpal bones from a sequence of 2D CT images using skeletally coupled deformable models. www.lem.s.brown.edu (2000).

[29] C. Xu and J. L. Prince. Snakes, Shapes , and Gradient Vector Flow. IEEE Trans. on Image Processing. 7, 3, (1988), 359—369.